IEEE Access
Multidisciplinary | Rapid Review | Open Access Journal

Received August 20, 2019, accepted August 30, 2019, date of publication September 9, 2019,
date of current version September 20, 2019.

Digital Object Identifier 10.1109/ACCESS.2019.2940049

A Modified Meander Line Microstrip Patch Antenna With Enhanced Bandwidth for 2.4 GHz ISM-Band Internet of Things (IoT) Applications

MOHAMMAD SHAHIDUL ISLAM[1], MOHAMMAD TARIQUL ISLAM[1], (Senior Member, IEEE), MD. AMANATH ULLAH[1], GAN KOK BENG[1], NOWSHAD AMIN[2], AND NORBAHIAH MISRAN[1]

[1]Center of Advanced Electronic and Communication Engineering, Universiti Kebangsaan Malaysia, Bangi 43600, Malaysia
[2]Institute of Sustainable Energy, Universiti Tenaga Nasional, Kajang 43000, Malaysia

Corresponding authors: Mohammad Shahidul Islam (P97645@siswa.ukm.edu.my) and Mohammad Tariqul Islam (tariqul@ukm.edu.my)

This work was supported by the University Research Grant under Project DIP-2018-018.

ABSTRACT Internet of Things (IoT) based application requires integration with the wireless communication technology to make the application data readily available. In this paper, a modified meander shape microstrip patch antenna has been proposed for IoT applications at 2.4 GHz ISM (Industrial, Scientific and Medical) band. The dimension of the antenna is $40\times10\times1.6$ mm^3. The antenna design is comprised of an inverse S-shape meander line connected with a slotted rectangular box. A capacitive load (C-load) and parasitic patch with the shaped ground are applied to the design. Investigations show that the antenna designed with an inverse S-shape patch and connecting rectangular box in the microstrip line has a higher efficiency and gain compare to the conventional meander shape antenna. The C-load is applied to the feed line to match the impedance. Moreover, parametric studies are carried out to investigate the flexibility of the antenna. Results show that, the gain and efficiency can be improved through adjusting the rectangular box with applying parasitic element and the shaped ground. The parasitic element has high impact on the bandwidth of the antenna of 12.5%. The finalized antenna has a peak gain of -0.256 dBi (measured) and 1.347 dBi (Simulated) with 79% radiation efficiency at 2.4 GHz. To prove the efficiency and eligibility in IoT applications, the measurement of the power delivered and received by the antenna at 2.4 GHz is performed and compared with the results of a dipole antenna. The antenna is integrated with 2.4 GHz radio frequency module and IoT sensors to validate the performance. The antenna novelty relies on the size compactness with high fractional bandwidth that is validated through the IoT application environment.

INDEX TERMS Internet of Things, meander line, capacitive load, parasitic patch, bandwidth.

I. INTRODUCTION

The Internet of Things (IoT) concept has now become an extension of the internet. It is a fast-growing worldwide network of interconnected variety of objects that supports many input-output devices, sensors and actuators based on standard communication protocol. Wireless sensor technology is contributing to improve the device connection to the internet as well as the efficiency of the IoT application operation [1]. Among all, antenna is playing an important role in wireless sensor technology that is heading towards a future with the explosive development of IoT techniques, increasing applications are found in various fields, including security, tracking, agriculture, smart city and smart home. Due to the high demand of multi-frequency and multi-function antenna in communication technologies, compact and easily integrated antenna design has received a vast amount of attention in the last few years [2]. The transmission of the merged communication data in the higher frequency is operated in the unlicensed industrial, scientific and medical 2.4 GHz band. A transparent loop antenna has been presented at [3] for IoT

The associate editor coordinating the review of this manuscript and approving it for publication was Sudipta Chattopadhyay.

applications where the antenna allows placement of itself at different places. A planar multi-standard MIMO antenna for IoT applications has also been developed at [4]. Loop antenna for biotelemetry IoT applications has been developed at [5] where it is used to operate in three standards: GSM 900, GSM 1800 and Bluetooth Low Energy (BLE). Wideband planar array antenna has been proposed for the radar applications where the radiation efficiency is measured 79.8% with 4.8 dBi realized gain at 2.4 GHz [6]. Planar patch antenna has also been presented at [7] for wireless communication systems with a high gain of 3.7 dBi and radiation efficiency of 73%. Leaky-wave antenna has been developed at [8] for scanning application of passive radar system where the fractional bandwidth is 136.5%. Planar antenna for GPS, Bluetooth and WiFi applications has been developed at [9] where the fractional bandwidth is 143.66% with omnidirectional radiation pattern. Thus, acceptable gain, bandwidth, radiation pattern, radiation efficiency etc., are the main challenges that need to be considered while designing microstrip patch antennas that operates in 2.4 GHz band [10]–[12].

Wireless Communication industry demands light and compact small antennas with low-cost fabrication [13]. In this case, a miniaturized meander shaped antenna is a suitable candidate as the space available for its installation is limited because it is introduced to achieve size reduction by implanting wire structure on a dielectric substrate [14]. A compact meandering slotted microstrip antenna has been proposed at [15] where it reduces the size of the antenna with a fixed frequency operation [16]. Besides, light and small antennas also reduce the bandwidth, gain and efficiency that is another challenge for communication technologies. Many techniques have been proposed by the researchers on enhancement of the gain, efficiency and bandwidth with satisfactory radiation characteristics by using meander shaped antennas. One of the important limitations of a microstrip antenna is single frequency and narrow bandwidth. A fork like tuning stub is applied to the microstrip slotted antenna to solve this issue [17]. A capacitive load (C-load) on 1.6 mm thick FR-4 substrate has been applied to enhance the peak gain with a fractional bandwidth of 7.23% and to improve the impedance matching which is a well-known technique for performance improvement [18], [19]. In addition, embedded meander line slits have been applied at [20] to enhance the fractional bandwidth. A technique to improve the bandwidth and gain is applying parasitic patch to the antenna. When parasitic patch is located closely to the fed patch, it increases the bandwidth and gain by about 3.3 dB [21]. Parasitic patch has been applied with inverted F-antenna to the mobile handsets for 2.4 GHz and the impedance bandwidth is 90 MHz [22]. Super bandwidth ranging from 2.90 to 20 GHz is obtained by applying disk shape monopole antenna with parasitic element [23]. Impedance matching has been improved by applying parasitic element where it works as director in the low operating band from 1.61-3.45 GHz [24]. Shaped ground has also been applied to the circular disk monopole antenna to match the impedance which is 50-ohm [25]. Impedance bandwidth also increases from 4.3% to 6% and 136% when applying parasitic element to the microstrip antenna at 2.99-3.10 GHz and 2.1-11.1GHz respectively [26], [27]. Various meander shaped antennas with different sizes have been proposed and measured for 2.4 GHz to get the good impedance fractional bandwidth [28]–[31].

This paper presents a modified meander shaped antenna for IoT applications at 2.4 GHz ISM band. The Computer Simulation Technology (CST) Microwave Studio simulator has been used for the simulation. The antenna is fabricated on a double-sided FR-4 printed circuit board for experimental measurements. In this design, a capacitive load is attached to the feed line with the meandered patch, which aids to achieve higher gain and bandwidth. It is shown that higher efficiency and bandwidth are also obtained by the parasitic patch with a shaped ground that keeps the gain static and increase the bandwidth. Furthermore, an experiment to measure the transmitted and received power using the antenna has been performed and the results are found to be in good agreement with similar experimental results of a dipole antenna.

II. ANTENNA DESIGN

The proposed meander shaped antenna (Figure 1) is designed on surface of low-cost FR-4 substrate (relative permittivity Er = 4.4, loss tangent = 0.02, and thickness of 1.6 mm). The antenna's size is $0.32\lambda \times 0.08\lambda$ with the ground plane of $0.25\lambda \times 0.08\lambda$, where λ is the wavelength at the operating frequency. The main radiator is a simple microstrip meander patch with two parallel lines that forms an inverse S-shape. The inverse S-shape connects to the last parallel line and forms a box shape B which is directly connected to the feed line. There is a C-load S connected to the feed line to match the impedance of 50-ohm and the impedance of the proposed antenna is 47-ohm. In addition, a parasitic element P that is incorporated at the right side of C-load and feed line to obtain impedance bandwidth. In order to clarify the effect of the shape B, C-load S and parasitic patch P, parametric study for different values of B, S and P are performed.

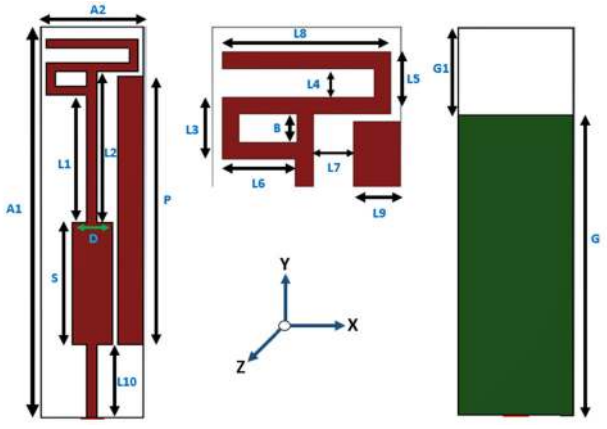

FIGURE 1. Antenna topology.

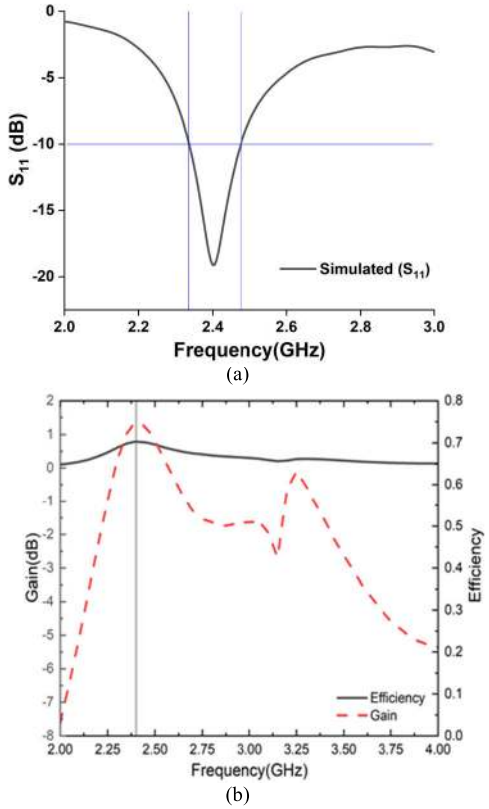

FIGURE 2. Simulated (a) reflection coefficient, (b) efficiency and gain of the proposed antenna.

Figure 2 represents the reflection coefficient, gain and efficiency of the prototype where the reflection coefficient at 2.4 GHz is −19.11 dB. The standard reflection coefficient is set −10 dB. Simulated pick gain is about 1.347 dB with 79% efficiency.

The design evolution of the proposed antenna is given step by step in Figure 3(a). Step 1 represents the basic antenna with a partial ground having a length of 31mm. In step 2, a capacitive load S is added into the meander line. A connecting patch B is added into the meander line in step 3. Finally, in step 4, a parasitic patch is added with the meander line. The reflection coefficient, efficiency and realized gain curve are given in Figure 3(b-d) which reflects the evolution of the proposed meander line antenna at 2.4GHz.

III. PARAMETER STUDY OF THE PROPOSED ANTENNA

Figure 4 and Figure 5 represent the parametric analysis of the different length of S which is started from 0.0 mm to 12.5 mm. The resonant frequency of antenna 1 shifted to the other frequency without the C-load (S = 0.0mm). Resonance frequency does not follow the reflection coefficient standard for antenna 2 to antenna 4. The proposed antenna achieves the target frequency 2.4 GHz through applying 12.5 mm size of S. The reflection coefficient also follows the standards that is less than −10 dB. Antenna 1 shows the higher efficiency and realized gain compared to proposed antenna, but

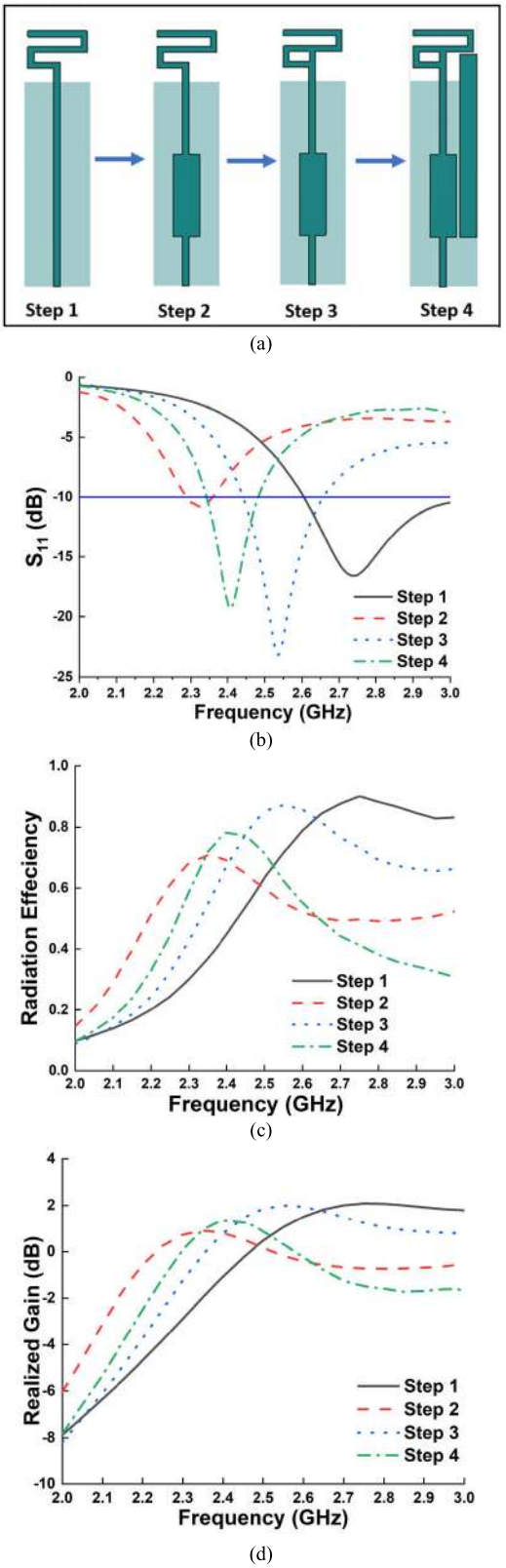

FIGURE 3. (a) Antenna evolution (b) reflection coefficient (c) efficiency (d) realized gain.

it does not have the expected resonance. Antenna 2 to antenna 4 shows the less efficiency and realized gain at the target resonance 2.4 GHz.

TABLE 1. Parameters of proposed antenna.

Substrate Length A	Ground G	L1	L2	L3	L4	L5	L6
40.0 mm	31.0 mm	13.0 mm	15.40 mm	3.30 mm	1.50 mm	3.30 mm	3.90 mm
Substrate Width A2	**G1**	**L7**	**L8**	**L9**	**L10**	**S**	**P**
10.0 mm	9.0 mm	2.10 mm	9.0 mm	2.50 mm	7.50 mm	12.50 mm	27.50 mm
		B	**D**				
		1.50 mm	4.00 mm				

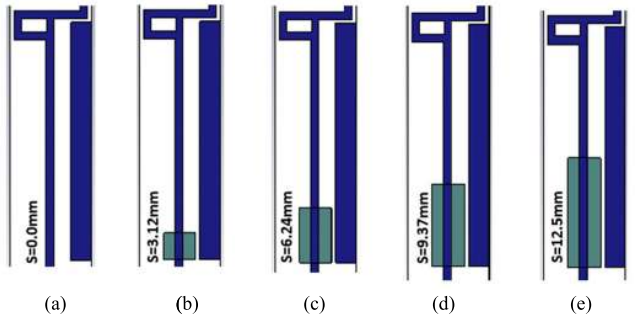

FIGURE 4. Parametric analysis of different C-load (a) antenna 1 (b) antenna 2 (c) antenna 3 (d) antenna 4 (e) proposed.

It is observed in Figure 7 that the parasitic patch has an impact on the reflection coefficient where it appears at 2.5 GHz for antenna 5 to antenna 7, but as the target is to achieve 2.4 GHz, P = 27.5mm is the obvious point for that target frequency. In this parametric, the width of the parasitic patch was static 2.5mm. The major noticeable point is the operational bandwidth. By applying the parasitic element with different lengths, antenna 5 to antenna 7 show the higher realized gain except the proposed length of 27.5 mm which sets the resonant frequency at 2.4 GHz. Figure 8 presents the efficiency curve in the context of width of parasitic patch. It is noticeable that the efficiency remains same for every different width at 2.4 GHz although the peak point of the efficiency moves slightly in context of changes. Thus, the effect of the parasitic patch is mostly depending on the length of it.

Figure 9 represents different shape of the structure B. Analysis that has an impact to the reflection coefficient is parametric of B shown in Table 2. It is observed that only the proposed antenna gets the target frequency 2.4 GHz with −19 dB reflection coefficient although antenna 8 and antenna 9 have the accepted reflection coefficient, but the frequency shifts to the other resonating points. The gain is much lower than the proposed antenna for antenna 8 and antenna 9.

Figure 10 represents different shape of ground plane of the proposed antenna. Table 3 represents the parametric analysis results of different ground shape. This analysis shows that the proposed antenna has the higher bandwidth and

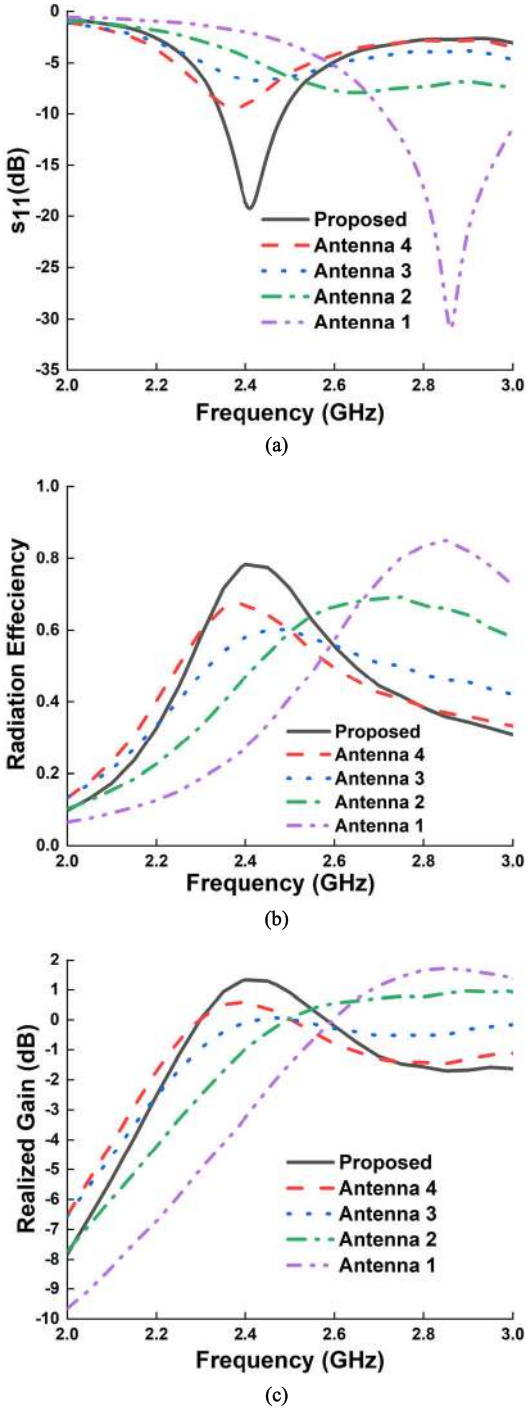

FIGURE 5. Parametric analysis of different C-load (a) reflection coefficient (b) efficiency (c) realized gain.

efficiency compared to ground shape of antenna 10, antenna 11 and antenna 12. Though antenna 10 and antenna 11 have a good reflection coefficient and gain, the proposed antenna ground has the target resonant frequency where the rest were shifted to different frequency. Thus, according to the results of the parametric numerical analysis, patches S = 12.5mm, B = 1.5mm, P = 27.5mm and ground with

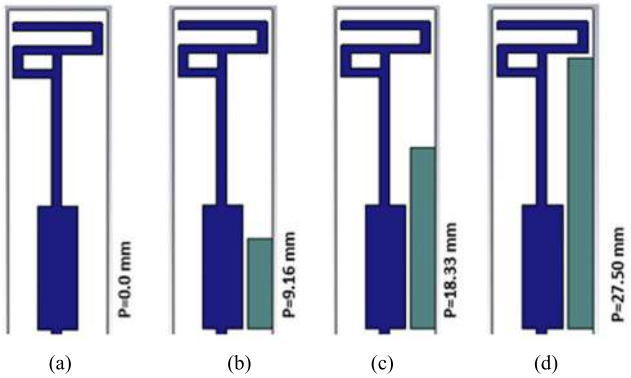

FIGURE 6. Parametric analysis of different length parasitic patch (a) antenna 5 (b) antenna 6 (c) antenna 7 (d) proposed.

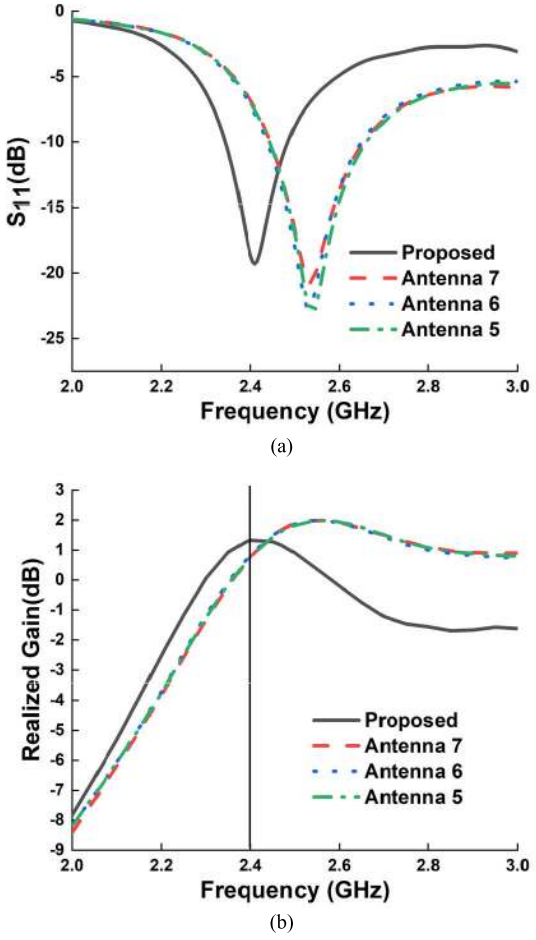

FIGURE 7. Parametric analysis of different length parasitic patch (a) reflection coefficient (b) realized gain of parasitic patch with different length.

G = 31mm were chosen for the final design and an antenna with these parameters has been fabricated. It is observed that the ground plane has a good impact on the impedance bandwidth. The bandwidth has enhanced when there is a shaped ground plane. On the contrast, the bandwidth mostly decreases with the changes of the length of ground plane structure.

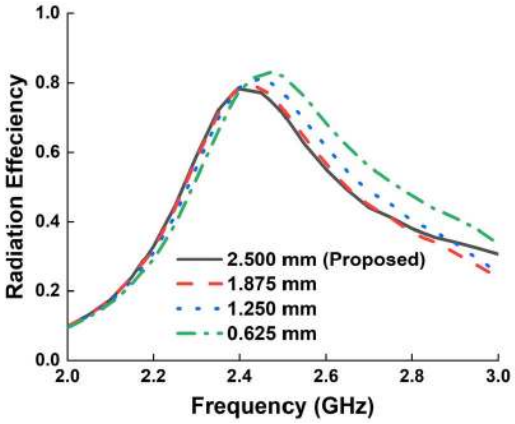

FIGURE 8. Parametric analysis of different width parasitic patch in context of efficiency.

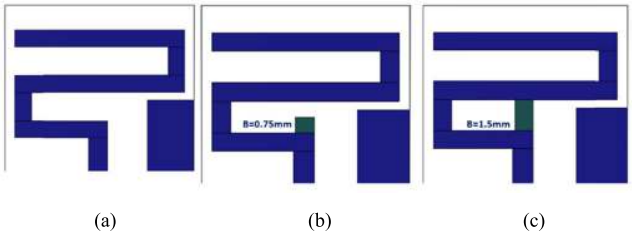

FIGURE 9. Parametric analysis of different B-Shape (a) antenna 8 (b) antenna 9 (c) proposed.

TABLE 2. Parametric analysis of B with the different length.

Properties	Proposed	Antenna 9	Antenna 8
Resonance Frequency (GHz)	2.40	2.25	2.25
S_{11} (dB)	-19.11	-15.12	-15.12
Bandwidth (MHz)	146	102	102
Radiation Efficiency	79	74	74
Realized Gain (dB)	1.347	-0.621	-0.621

IV. SURFACE CURRENT AND EQUIVALENT LUMPED CIRCUIT MODEL ANALYSIS

The current distribution of the antenna at 2.4 GHz is shown in Figure 11. The interspersion of the box shaped radiator helps to achieve a dominating current in the modified meander line radiator, increasing the effective radiating length. Also, significant current exists on the feed radiator from the capacitive load. The radiating element in the meander antenna shows that majority of the current distribution is concentrated around the portion of the C-load to the meandered radiating element, making it the main radiator. However, the current distribution of the parasitic patch is high on the left side of the parasitic element aiding the resonance of the antenna by shifting it at 2.4 GHz and the extended upper part of C load impacts the antenna in context of gain enhancement because of the appearance of the high current on the upper part.

TABLE 3. Parametric analysis of ground plane with the different length.

Properties	Antenna 10	Proposed	Antenna 11	Antenna 12
Frequency (GHz)	4.06	2.40	2.34	2.3
S_{11} (dB)	-27.19	-19.11	-20.74	-8.5
Bandwidth (MHz)	69	146	114	Not Applicable (Below -10dB)
Radiation Efficiency	07	79	79	71
Realized Gain (dB)	-7.3	1.347	1.35	0.73

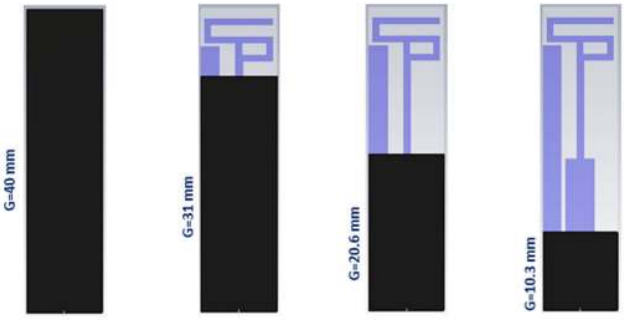

FIGURE 10. Parametric analysis of different ground shape (a) antenna 10 (b) proposed (c) antenna 11 (d) antenna 12.

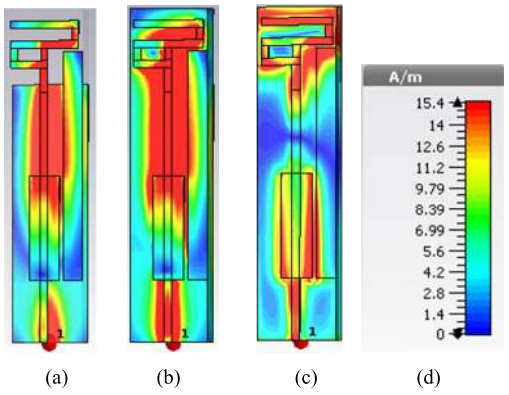

FIGURE 11. Simulated current distribution of the optimized antenna (a) surface current (b) H-field (c) E-field (d) scale.

The proposed antenna has been developed in terms of the transmission line principle where a single patch represents as a series RLC circuit. This type of structure postures passive LC circuit that interact with resonance frequency, which is denoted by the following equation,

$$f = \frac{1}{\pi\sqrt{\mathrm{LC}}} \tag{1}$$

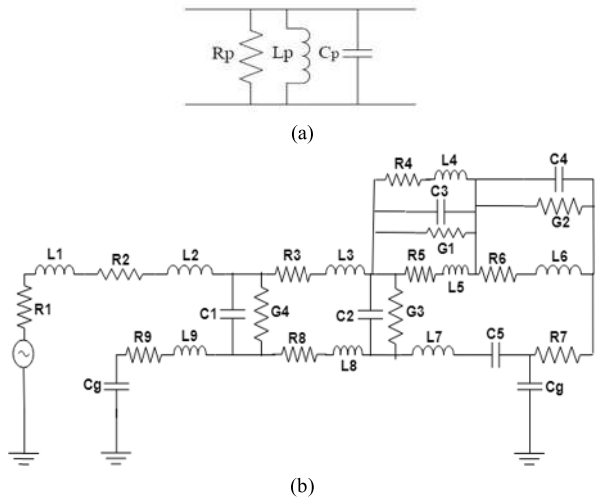

FIGURE 12. Equivalent Lump circuit model for (a) Normal patch antenna (b) Proposed antenna.

where L denotes the lumped inductance and C denotes the lumped capacitance. The split inside the metal loop represents capacitance and the metal loop itself form inductance.

The combination of the split and electric field generates electric resonance, on the other hand, the magnetic fields and the metal loops form magnetic resonances while applying the electromagnetic wave propagation through the structure. The formation of capacitance between the split can be explained with the following equation,

$$C = \varepsilon_0 \varepsilon_r \frac{A}{d}(F) \tag{2}$$

Here, $\varepsilon 0$ represents free space and εr is relative permittivity, the area of the split is A and d stands for the split length which is "g" in the proposed structure. The equivalent inductance is calculated according to the transmission line principle mentioned in [2].

$$L(nH) = 2 \times 10^{-4} l \left[\ln\left(\frac{l}{w+t}\right) + 1.193 + 0.02235\frac{w+t}{l} \right] K_g \tag{3}$$

where, l = length of microstrip line, w = width of microstrip line, t = thickness of microstrip line, correction factor = Kg $= 0.57 - 0.145 \ln\frac{w'}{h'}$, h' means the thickness of the substrate and w' means the width of the substrate. Both the external and internal inductance must be considered to determine the total inductance.

Figure 12 (a) represents the equivalent electrical modeling of ordinary rectangular patch antenna that can be designed as parallel RLC components based on cavity model. Figure 10 (b) represents the equivalent lumped circuit model for the proposed patch antenna where an inductor for the metal strip and capacitors for the gaps have been included. The strips that form magnetic inductance can be considered as inductors and the capacitance are formed in and around the strip gaps. The changes in the capacitance 'C' and inductance

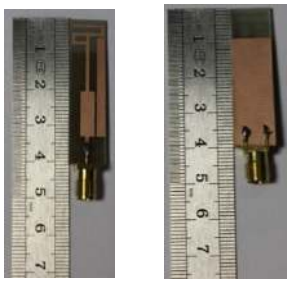

FIGURE 13. Fabricated antenna (a) patch (b) ground.

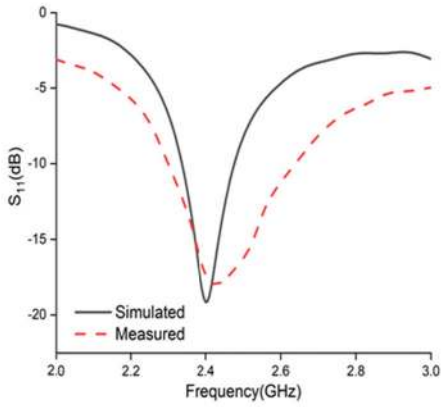

FIGURE 14. Reflection coefficient of the prototype.

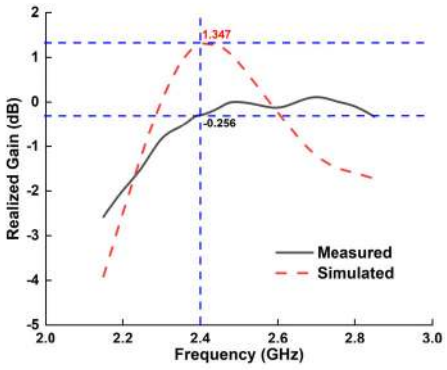

FIGURE 15. Measured and simulated realized gain.

'L' due to the dielectric loading leads to considerable shift in the frequency of resonance. In this model, the combination of L1 to L9 and C1 to C5 represents the equivalent lumped model of the feed line, C-load, B-shape, parasitic patch and shaped ground. R1 to R7 and G1 to G4 represents the equivalent resistance in series and parallel form of the equivalent lumped circuit model. L1 represents the feed line and L2 represents the C-load of the proposed antenna where L9 represents the parasitic patch. The gap between them creates the capacitance C1. L3, L4, L5 and L6 are the patch of the proposed antenna where the gaps between L4 and L5 creates capacitance C3. C4 emerges due to the gap among L3, L4 and L5. L7 and L8 also represent the parasitic patch and create capacitance C2 and C5 due to the gap between patch and parasitic element. As the top and bottom conducting

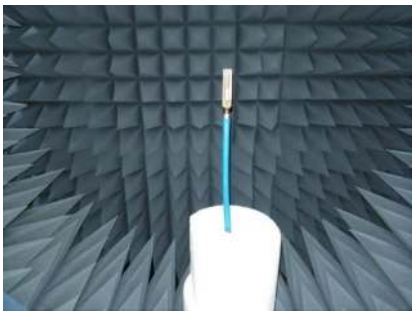

FIGURE 16. Radiation pattern measurement.

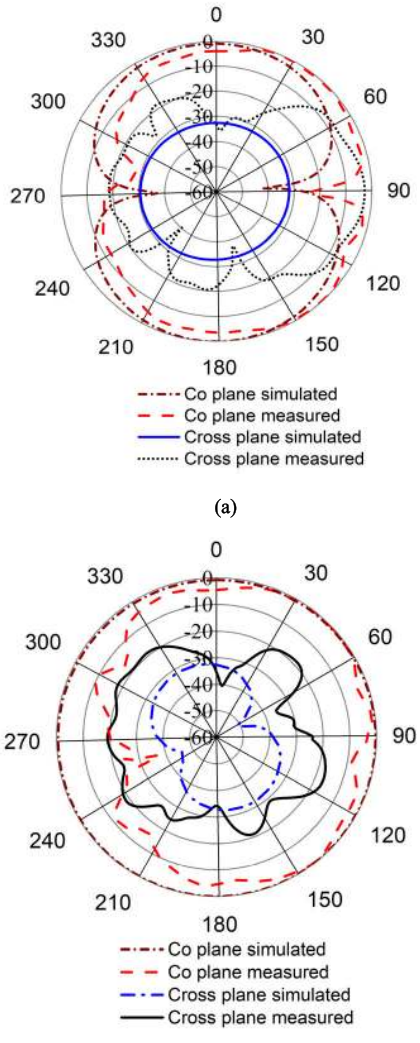

FIGURE 17. Simulated and measured radiation patterns of the proposed antenna at 2.4 GHz (a) E Plane (b) H Plane.

layers are separated by a dielectric material FR4, capacitance emerges between the patch and ground plane and it is named as Cg which creates capacitance due to the gap between patch and shaped ground.

V. RESULTS AND DISCUSSION

The proposed antenna was fabricated and validated by measurement. Figure 13 represents the fabricated antenna.

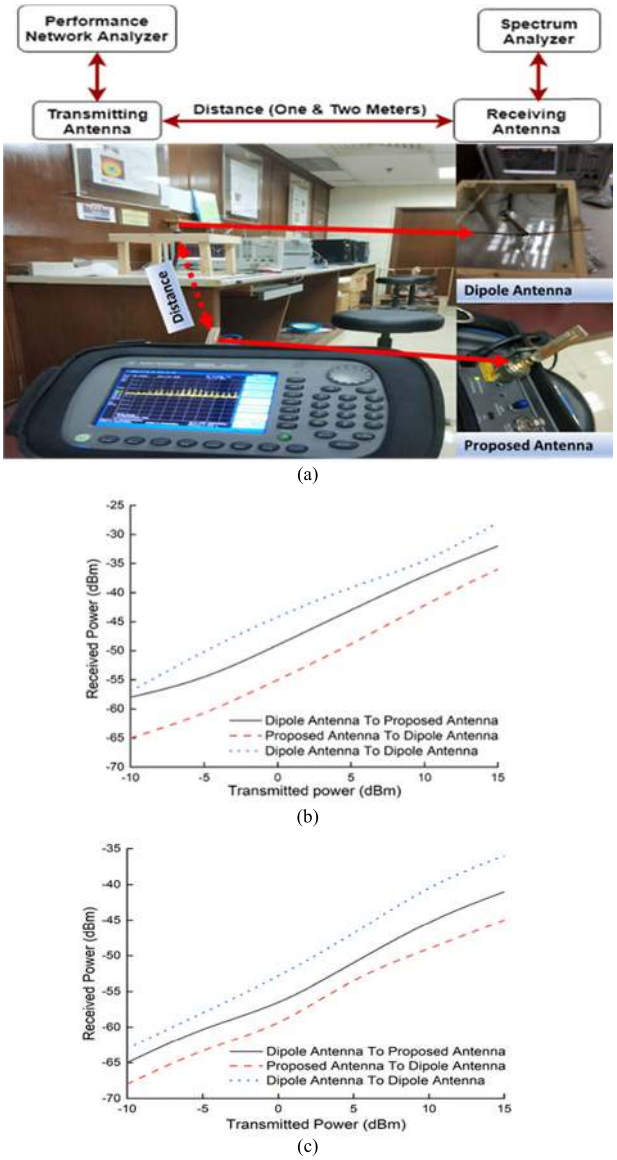

FIGURE 18. **(a) Block diagram of antenna power transmission and receiving with dipole and proposed antenna (b) data of power received and transmitted using the antenna with respect to distance between Rx and Tx for one-meter (c) data of power received and transmitted using the antenna with respect to distance between Rx and Tx for Two-meter.**

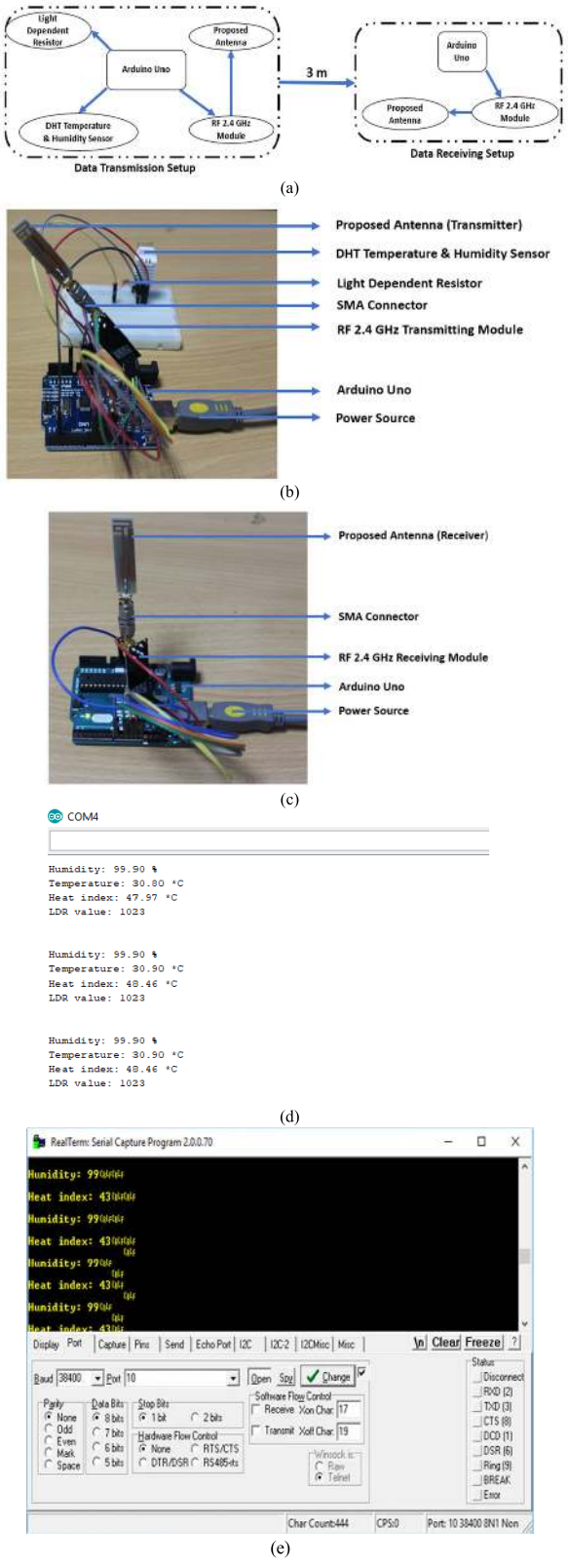

FIGURE 19. **(a) System setup (b) data transmission setup (c) data receiving setup (d) data transmission (e) data receiving.**

An SMA connector was used at the input port to feed the radiator. During the antenna measurements, a power network analyzer (PNA-E8362C 10 MHz-67 GHz) was used to measure the input impedance of the prototype. The measured and simulated reflection coefficients for the proposed antenna are shown in Figure 14. The simulated impedance bandwidth for $|S11| < -10$ dB was 146 MHz (2.336 – 2.482 GHz), whereas the measured result was 300 MHz (2.35-2.65 GHz) which is almost double of the simulated result. However, simulated and measured results are in good agreement, though a little mismatch is observed in the bandwidth. The main reasons of the mismatch between two results are fabrication tolerance and deficient soldering effects of the SMA connector. Moreover, this bandwidth disagreement may be occurred due to RF feeding cable, which was not considered in simulation. Figure 15 shows the simulated and measured realized gain of the proposed antenna where the measured realized gain

TABLE 4. Performance comparison for the state of microstrip meander antenna at 2.4 GHz.

Reference	Year	Antenna Shape	Antenna Size (mm^2)	Fractional Bandwidth (%)	Gain (dB)	Intended Applications	Antenna Applied to the Application	Remarks (Compared with Proposed Antenna)
[13]	2014	Meander Line Monopole	32x1.6	7.6	0.5	Not Specified	No	Lower bandwidth and Gain
[18]	2017	Meander	26x15.6	7.23	4.49	Not Specified	No	Lower bandwidth
[28]	2011	Meander-line	60x20	12.5	3.15	USB WLAN	No	Enhanced Size and similar bandwidth
[29]	2016	Meander Line	30x20	10	Not Specified	WLAN Applications	No	Enhanced Size and lower bandwidth
[30]	2013	Meander-line Monopole	60x20	11	1.6	Wireless Communications	No	Enhanced Size and lower bandwidth
[32]	2019	Quarter Circle with Rectangular Section	38x10.8	11.5	1.97	Wireless Application	No	Lower bandwidth
[33]	2003	Double-T Monopole	70x50	3.43	1.3	WLAN Operations	No	Enhanced Size, lower bandwidth & gain
[34]	2004	Rectangular Slot	75x75	10.6	3.7	Wireless Communication	No	Enhanced Size and lower bandwidth
[35]	2018	Uniplanar Meandered	10x19	8	1.2	2.5 GHz Applications	No	Lower bandwidth and Gain
[36]	2017	Twin Spiral Slot	12.45x13.05	7.5	1.33	Not Specified	No	Lower bandwidth and Gain
[37]	2014	Inverted L-shape	25x30	3.43	2.1	TD-LTE and WLAN Applications	No	Enhanced Size and lower bandwidth
[38]	2019	MIMO Patch	52.3x128	8	2.56	Not Specified		Enhanced Size and lower bandwidth
[39]	2018	Folded Dipole	110x68	14.23	3.02	GPS/DCS/WLAN/WiMax Application	No	Enhanced Size and lower bandwidth
[40]	2018	$ shape	100x40	3.3	Not Specified	WLAN APPlications	No	Enhanced Size and lower bandwidth
[4]	2018	MIMO	120x65	54.92	2.85	Internet of Things Application	Yes	Enhanced Size
Proposed Antenna	**2019**	**Meander Line Microstrip Patch**	**40x10**	**12.5**	**-0.256 (Measured) +1.347 (Simulated)**	**Internet of Things Applications**	**Yes**	**Small size with high bandwidth.**

is −0.256 dB which has achieved a satisfactory gain as it is a very small in size. The slight discrepancy between simulated and measured gain at the operating frequency may have been arise due to the utilization of the blue cable and connector during the measurement, shown in Figure 15. The extra cable and connector used for measuring the gain have not been considered in simulation.

The antenna radiation pattern has been performed in the SATIMO anechoic chamber depicted in Figure 16. The simulated and measured radiation patterns of the proposed antenna for $\varphi = 0°$ and $\varphi = 90°$ at 2.4 GHz are shown in Figure 17(a) as E plane and Figure 17(b) as H plane. The antenna achieved omnidirectional radiation patterns at $\varphi = 90°$ and bidirectional patterns at $\varphi = 0°$ plane. The cross-polarization level is negligible in both planes. An experiment has been conducted to measure the power of received signal using the proposed antenna. The experiment setup is shown in Figure 16. Performance Network Analyzer (PNA-E8362C 10 MHz-67 GHz) has been used as signal generator to transfer signal at 2.4 GHz using the transmitting antenna and Spectrum Analyzer (N9342C 100 kHz-7 GHz) has been used to measure the received power at 2.4 GHz. Initially, power received by

a dipole antenna from another dipole antenna at 2.4 GHz is taken as reference. 10 dB and 20 dB attenuation have been applied at the transmitting and receiving end. The data of received power has also been obtained varying the distance between transmitting and receiving antenna (one-meter and two-meter). For analyzing the result, the transmitted power is set from −10 dBm to +15 dBm gradually. Values of transmitted and received power of dipole to proposed antenna (D-P), proposed to dipole antenna (P-D) and dipole to dipole antenna (D-D) are shown in Figure 16. The value of received power are −57 dBm, −58 dBm and −65 dBm for D-P, P-D, and D-D respectively when the distance between transmitting and receiving antenna is one-meter and transmitted power is −10 dBm, depicted in Figure 18 (a). When the transmitted power is +15 dBm, at the receiving end −32dBm, −36 dBm and −28 dBm power are observed. Figure 18 (b) represents the data of transmitted and received power when the distance of transmitter and receiver is two-meter. It shows the received power values are −65 dBm, −68 dBm and −63 dBm respectively for D-P, P-D, and D-D configuration at −10 dBm transmitted power. By analyzing the received and transmitted power in terms of distance, it is observed that the receiving power is decreasing for D-P, P-D and D-D as the distance is increased. However, the data of power transmitted and received are close to the data of the reference configuration D-D with approximately 2-5 dBm variation.

Figure 19 (a) shows the block diagram of experimental setup of the proposed antenna which is performed by Arduino microcontroller and radio frequency module at 2.4 GHz. The data transmission setup contains the DHT temperature, humidity and heat index sensor, light dependent resistor and the proposed antenna as a transmitter which is shown in Figure 19 (b). On the other side, the proposed antenna has been set up as a receiver connected with the Arduino Uno which is shown in Figure 19 (c). The distance between transmission and receiving antenna has been set three meter which is performed in a room temperature. The proposed antenna is successful in terms of receiving the sensor data and sending to the other antenna. The receiving sensor data is given at Figure 19 (d) and the transmitted result data has been shown in Figure 19 (e) which has been performed by applying the Realterm hyper-terminal application tool by setting up the specific port and baud rate.

Table 4 compares the proposed antenna with the existing microstrip antenna for 2.4 GHz. Many researchers have presented many structures of the antenna for 2.4 GHz with parametric and measurement results for different applications. The comparison shows that the proposed antenna has the higher fractional bandwidth compared to all except the design presented by Park et al. It is noticeable from the comparison table that the existing antenna sizes which are mostly larger than the proposed antenna have lower fractional bandwidth. The gain is another issue with the proposed antenna. The simulated gain of the proposed antenna is higher in some cases compare to the existing ones although it has lower measured realized gain due to the utilization of the blue cable and connector during the measurement. In addition, most of the presented antennas are developed for an intended application but the implementation or testing for that specification have not done properly. Compare to that, the proposed antenna has been used in the real time IoT application to verify the performance at 2.4 GHz. Thus, with reference to the table, the performance of the proposed antenna is more compatible than others which is an acceptable solution for 2.4 GHz IoT applications.

VI. CONCLUSION

Applying antenna as a wireless sensor technology is one the advantages in IoT applications. In this paper, we presented a modified microstrip meander line antenna for the 2.4 GHz ISM band which is a potential solution to apply in IoT based applications. The performances of inverse S-shape, rectangular box, capacitive load and parasitic patch were investigated numerically and validated with measurements result. The parametric analysis of the ground plane was also investigated, and it came up with a shaped ground. Results demonstrated that, due to applying rectangular box and shaped ground plane, the antenna came with a good efficiency and positive simulated gain of 1.347 dB. It was also noticeable that the capacitive load keeps the gain and efficiency static and it was an appropriate solution for impedance matching. Parasitic patch applying to the antenna creates the higher fractional bandwidth of 12.5% which has got the special attention when it is compared to other conventional antennas. In addition, the antenna has been used as a transmitter and receiver to verify the eligibility and efficiency of the antennas' performance for the intended IoT applications by observing the transmitted and received power of the antenna. Finally, the antenna is validated through applying to radio frequency module and IoT sensors at 2.4 GHz.

REFERENCES

[1] M. S. Islam, M. T. Islam, A. F. Almutairi, G. K. Beng, N. Misran, and N. Amin, "Monitoring of the human body signal through the Internet of Things (IoT) based LoRa wireless network system," *Appl. Sci.*, vol. 9, no. 9, p. 1884, 2019.

[2] A. Alomainy, Y. Hao, and F. Pasveer, "Numerical and experimental evaluation of a compact sensor antenna for healthcare devices," *IEEE Trans. Biomed. Circuits Syst.*, vol. 1, no. 4, pp. 242–249, Dec. 2007.

[3] Y. Koga and M. Kai, "A transparent double folded loop antenna for IoT applications," in *Proc. IEEE-APS Top. Conf. Antennas Propag. Wireless Commun. (APWC)*, Sep. 2018, pp. 762–765.

[4] K. R. Jha, B. Bukhari, C. Singh, G. Mishra, and S. K. Sharma, "Compact planar multistandard MIMO antenna for IoT applications," *IEEE Trans. Antennas Propag.*, vol. 66, no. 7, pp. 3327–3336, Jul. 2018.

[5] H. A. Damis, N. Khalid, R. Mirzavand, H.-J. Chung, and P. Mousavi, "Investigation of epidermal loop antennas for biotelemetry IoT applications," *IEEE Access*, vol. 6, pp. 15806–15815, 2018.

[6] M. Alibakhshikenari, B. S. Virdee, and E. Limiti, "Wideband planar array antenna based on SCRLH-TL for airborne synthetic aperture radar application," *J. Electromagn. Waves Appl.*, vol. 32, no. 12, pp. 1586–1599, 2018.

[7] M. Alibakhshikenari, B. S. Virdee, A. Ali, and E. Limiti, "Miniaturised planar-patch antenna based on metamaterial L-shaped unit-cells for broadband portable microwave devices and multiband wireless communication systems," *IET Microw., Antennas Propag.*, vol. 12, no. 7, pp. 1080–1086, 2018.

[8] M. Alibakhshikenari, B. S. Virdee, A. Ali, and E. Limiti, "A novel monofilar-archimedean metamaterial inspired leaky-wave antenna for scanning application for passive radar systems," *Microw. Opt. Technol. Lett.*, vol. 60, no. 8, pp. 2055–2060, Aug. 2018.

[9] M. Alibakhshikenari, E. Limiti, M. Naser-Moghadasi, B. S. Virdee, and R. A. Sadeghzadeh, "A new wideband planar antenna with band-notch functionality at GPS, Bluetooth and WiFi bands for integration in portable wireless systems," *AEU-Int. J. Electron. Commun.*, vol. 72, pp. 79–85, Feb. 2017.

[10] C. Liu, Y.-X. Guo, and S. Xiao, "A hybrid patch/slot implantable antenna for biotelemetry devices," *IEEE Antennas Wireless Propag. Lett.*, vol. 11, pp. 1646–1649, 2012.

[11] M. Ullah, M. T. Islam, T. Alam, and F. B. Ashraf, "Paper-based flexible antenna for wearable telemedicine applications at 2.4 GHz ISM band," *Sensors*, vol. 18, no. 12, p. 4214, 2018.

[12] M. Samsuzzaman, T. Islam, N. H. Abd Rahman, M. R. I. Faruque, and J. S. Mandeep, "Compact modified swastika shape patch antenna for WLAN/WiMAX applications," *Int. J. Antennas Propag.*, vol. 2014, Apr. 2014, Art. no. 825697.

[13] M. W. K. Lee, K. W. Leung, and Y. L. Chow, "Low cost meander line chip monopole antenna," *IEEE Trans. Antennas Propag.*, vol. 62, no. 1, pp. 442–445, Jan. 2014.

[14] F. B. Ashraf, T. Alam, S. Kibria, and M. T. Islam, "A compact meander line elliptic split ring resonator based metamaterial for electromagnetic shielding," *Mater. Express*, vol. 8, no. 2, pp. 133–140, 2018.

[15] J.-S. Kuo and K.-L. Wong, "A compact microstrip antenna with meandering slots in the ground plane," *Microw. Opt. Technol. Lett.*, vol. 29, no. 2, pp. 95–97, 2001.

[16] M. T. Islam, M. Cho, M. Samsuzzaman, and S. Kibria, "Compact antenna for small satellite applications [antenna applications corner]," *IEEE Antennas Propag. Mag.*, vol. 57, no. 2, pp. 30–36, Apr. 2015.

[17] S. Sadat, M. Fardis, F. Geran, G. Dadashzadeh, N. Hojjat, and M. Roshandel, "A compact microstrip square-ring slot antenna for UWB applications," in *Proc. IEEE Antennas Propag. Soc. Int. Symp.*, Jul. 2006, pp. 4629–4632.

[18] J.-H. Chen, C.-K. Yang, C.-Y. Cheng, C.-C. Yu, and C.-H. Hsu, "Gain enhancement of a compact 2.4-GHz meander antenna using inductive feed and capacitive load," *Microw. Opt. Technol. Lett.*, vol. 59, no. 10, pp. 2598–2604, 2017.

[19] F. Aznar-Ballesta, J. Selga, P. Vélez, A. Fernández-Prieto, J. Coromina, J. Bonache, and F. Martín, "Slow-wave coplanar waveguides based on inductive and capacitive loading and application to compact and harmonic suppressed power splitters," *Int. J. Microw. Wireless Technol.*, vol. 10, nos. 5–6, pp. 530–537, 2018.

[20] M. Alibakhshi-Kenari, M. Naser-Moghadasi, R. A. Sadeghzadeh, B. S. Virdee, and E. Limiti, "Bandwidth extension of planar antennas using embedded slits for reliable multiband RF communications," *AEU-Int. J. Electron. Commun.*, vol. 70, no. 7, pp. 910–919, 2016.

[21] B. Yildirim and B. A. Cetiner, "Enhanced gain patch antenna with a rectangular loop shaped parasitic radiator," *IEEE Antennas Wireless Propag. Lett.*, vol. 7, pp. 229–232, 2008.

[22] Y. J. Cho, S. H. Hwang, and S. O. Park, "A dual-band internal antenna with a parasitic patch for mobile handsets and the consideration of the handset case and battery," *IEEE Antennas Wireless Propag. Lett.*, vol. 4, no. 1, pp. 429–432, Sep. 2005.

[23] M. M. Islam, M. T. Islam, M. R. I. Faruque, N. Misran, M. Samsuzzaman, M. I. Hossain, and T. Alam, "A compact disc-shaped super wideband patch antenna with a structure of parasitic element," *Int. J. Appl. Electromagn. Mech.*, vol. 50, no. 1, pp. 11–28, 2016.

[24] L. Chang, L. L. Chen, J. Q. Zhang, and D. Li, "A broadband dipole antenna with parasitic patch loading," *IEEE Antennas Wireless Propag. Lett.*, vol. 17, no. 9, pp. 1717–1721, Sep. 2018.

[25] J. Liang, C. C. Chiau, X. Chen, and C. G. Parini, "Study of a printed circular disc monopole antenna for UWB systems," *IEEE Trans. Antennas Propag.*, vol. 53, no. 11, pp. 3500–3504, Nov. 2005.

[26] J.-F. Lin and Q.-X. Chu, "Enhancing bandwidth of CP microstrip antenna by using parasitic patches in annular sector shapes to control electric field components," *IEEE Antennas Wireless Propag. Lett.*, vol. 17, no. 5, pp. 924–927, May 2018.

[27] S. T. Fan, Y. Z. Yin, B. Lee, W. Hu, and X. Yang, "Bandwidth enhancement of a printed slot antenna with a pair of parasitic patches," *IEEE Antennas Wireless Propag. Lett.*, vol. 11, pp. 1230–1233, 2012.

[28] E. G. Lim, Z. Wang, S. Zhang, and Y. Jiang, "Compact USB WLAN Printed Meander Line Antennas," *Procedia Eng.*, vol. 15, pp. 2516–2520, Jan. 2011.

[29] A. Pandey, C. Singhania, and R. Mishra, "Design of a compact dual band meandering line monopole antenna for WLAN 2.4/5.0 GHz applications," in *Proc. Int. Conf. Signal Process., Commun., Power Embedded Syst. (SCOPES)*, Oct. 2016, pp. 830–833.

[30] C. C. Hsu and H. H. Song, "Design, fabrication, and characterization of a dual-band electrically small meander-line monopole antenna for wireless communications," *Int. J. Electromagn. Appl.*, vol. 3, no. 2, pp. 27–34, 2013.

[31] M. Samsuzzaman, M. Rokunuzzaman, S. K. Thian, and M. T. Islam, "A new design of bracket shape dipole and meander line UHF RFID tag," *Acta Technica CSAV (Ceskoslovensk Akademie Ved)*, vol. 62, no. 3, pp. 221–230, 2017.

[32] M. Koohestani, J. Tissier, and M. Latrach, "A compact wideband ACS-fed monopole antenna for wireless applications around 2.45 GHz," in *Proc. 13th Eur. Conf. Antennas Propag. (EuCAP)*, Mar./Apr. 2019, pp. 1–3.

[33] Y.-L. Kuo and K.-L. Wong, "Printed double-T monopole antenna for 2.4/5.2 GHz dual-band WLAN operations," *IEEE Trans. Antennas Propag.*, vol. 51, no. 9, pp. 2187–2192, Sep. 2003.

[34] J. W. Wu, H. M. Hsiao, J. H. Lu, and S. H. Chang, "Dual broadband design of rectangular slot antenna for 2.4 and 5 GHz wireless communication," *Electron. Lett.*, vol. 40, no. 23, pp. 1461–1463, Nov. 2004.

[35] P. V. Naidu, A. Kumar, and R. Rajkumar, "Design, analysis and fabrication of compact dual band uniplanar meandered ACS fed antenna for 2.5/5 GHz applications," *Microsyst. Technol.*, vol. 25, no. 1, pp. 97–104, 2019.

[36] W. Liu, L. Xu, and H. Zhan, "Design of 2.4 GHz/5 GHz planar dual-band electrically small slot antenna based on impedance matching circuit," *AEU-Int. J. Electron. Commun.*, vol. 83, pp. 322–328, Jan. 2018.

[37] S. Chen, D. Dong, Z. Liao, Q. Cai, and G. Liu, "Compact wideband and dual-band antenna for TD-LTE and WLAN applications," *Electron. Lett.*, vol. 50, no. 16, pp. 1111–1112, 2014.

[38] M. Chanda, K. Sarmah, S. Goswami, and K. K. Sarma, "2×1 MIMO antenna at 2.4 GHz with improved isolation," in *Proc. 6th Int. Conf. Signal Process. Integr. Netw. (SPIN)*, 2019, pp. 1008–1013.

[39] J. Park, M. Jeong, N. Hussain, S. Rhee, P. Kim, and N. Kim, "Design and fabrication of triple-band folded dipole antenna for GPS/DCS/WLAN/WiMAX applications," *Microw. Opt. Technol. Lett.*, vol. 61, no. 5, pp. 1328–1332, 2019.

[40] T. Srivastava, S. Saurabh, A. Vyas, and R. Mishra, "A triple band $ shape slotted PIFA for 2.4 GHz and 5 GHz WLAN applications," in *Soft Computing: Theories and Applications*. Singapore: Springer, 2019, pp. 399–406.

MOHAMMAD SHAHIDUL ISLAM was born in Brahmanbaria, Bangladesh, in 1993. He received the B.Tech. degree (Hons.) in software engineering from Infrastructure University Kuala Lumpur, in 2018. He is currently pursuing the M.Sc. degree in electrical and electronic engineering with the Universiti Kebangsaan Malaysia (UKM), Malaysia, where he is also a Graduate Research Assistant with the Center of Advanced Electronic and Communication Engineering. He has authored or couthored a number of referred journals and conference articles. His current research interests include the Internet of Things, antenna and wave propagation, wireless communication, and metamaterials.

MOHAMMAD TARIQUL ISLAM is currently a Professor with the Department of Electrical, Electronic and Systems Engineering, Universiti Kebangsaan Malaysia (UKM), and a Visiting Professor with the Kyushu Institute of Technology, Japan. He is the author and coauthor of about 475 research journal articles, nearly 175 conference articles, and a few book chapters on various topics related to antennas, microwaves, and electromagnetic radiation analysis with 18 inventory patents filed. His publications have been cited 5100 times and his H-index is 37 (Source: Scopus). His Google scholar citation is 6800 and H-index is 39. His current research interests include communication antenna design, radio astronomy antennas, satellite antennas, and electromagnetic radiation analysis. Dr. Islam currently serves as the Guest Editor of *Sensors* Journal, an Associate Editor of IEEE Access and *IET Electronics Letter*. He was a recipient of more than 40 research grants from the Malaysian Ministry of Science, Technology and Innovation, Ministry of Education; UKM research grant; and international research grants from Japan and Saudi Arabia. He received several International Gold Medal awards, the Best Invention in Telecommunication Award, the Special Award from Vietnam for his research and innovation, and the Best Researcher Awards from UKM, in 2010 and 2011, respectively. He was a recipient of the 2018 IEEE AP/MTT/EMC Excellent Award. He also received the Best Innovation Award, in 2011, and the Best Research Group in ICT niche from UKM, in 2014. He was a recipient of the Publication Award from Malaysian Space Agency, in 2009, 2010, 2013, and 2014, and the Best Paper Presentation Award from the 2012 International Symposium on Antennas and Propagation (ISAP 2012), Nagoya, Japan, and from the 2015 IconSpace. He is a Chartered Professional Engineer-CEng, and a member of IET, U.K., and IEICE, Japan.

MD. AMANATH ULLAH was born in Chittagong, Bangladesh, in 1993. He received the B.Sc. degree in electrical and electronic engineering (EEE) from International Islamic University Chittagong (IIUC), in 2015. He is currently pursuing the M.Sc. degree in electrical, electronic and systems engineering with the Universiti Kebangsaan Malaysia (UKM). He published over nine research journal articles, nearly nine conference articles, and one book chapters on various topics related to antennas, microwaves, and electromagnetic radiation analysis. His current research interests include antenna and propagation, 3D antenna applications, small satellite antenna, microwave imaging, and embedded systems.

GAN KOK BENG was born in Malaysia, in 1978. He received the B.S. degree in material physics from the University Technology Malaysia, in 2001. He was an Optical-Design Engineer, from 2003 to 2005. He is currently an Associate Professor with the Centre of Advanced Electronic and Communication Engineering (PAKET), Universiti Kebangsaan Malaysia. His current research interests include embedded system in healthcare and biomechanics and human motion analysis.

NOWSHAD AMIN served over 11 years with the Department of Electrical, Electronic and Systems Engineering, Universiti Kebangsaan Malaysia, from 2006 to 2018, where he led the Solar Photovoltaic Research Group under the Solar Energy Research Institute (SERI). He is currently a Strategic Hire Professor with the Institute of Sustainable Energy, Universiti Tenaga Nasional, Malaysia, and an adjunct to the Faculty of Engineering and Built Environment, Universiti Kebangsaan Malaysia (UKM).

NORBAHIAH MISRAN received the B.Eng. degree in electrical, electronic, and systems engineering from the Universiti Kebangsaan Malaysia (UKM), in 1999, and the Ph.D. degree from the Queen's University of Belfast, Northern Ireland, U.K., in 2004. She started her career as a Tutor, in 1999. Later, she has been appointed as a Lecturer, in 2004, and an Associate Professor, in 2009. She is currently a Professor with UKM. Her current research interest includes RF device design, particularly, in broadband microstrip antennas, reconfigurable antennas, and reflect array antennas. She is also conducting some researches in the engineering education field.